Hindawi
Advances in Materials Science and Engineering
Volume 2020, Article ID 9016583, 13 pages
https://doi.org/10.1155/2020/9016583

Research Article

Analysis of Resistivity Anisotropy of Loaded Coal Samples

Xiangchun Li,[1,2,3] Zhenxing An,[1] Qi Zhang,[1] Xiaolong Chen,[1] Xinwei Ye,[1] and Suye Jia[1]

[1]*School of Emergency Management and Safety Engineering, China University of Mining & Technology, Beijing 100089, China*
[2]*State Key Laboratory of Coal Resources and Safe Mining, Beijing 100083, China*
[3]*State Key Laboratory Cultivation Base for Gas Geology and Gas Control, Jiaozuo 454000, China*

Correspondence should be addressed to Zhenxing An; anzhenxingz@163.com

Received 6 December 2019; Accepted 11 May 2020; Published 4 June 2020

Academic Editor: Candido Fabrizio Pirri

In this paper, an experimental study of the variation of resistivity of coal samples in different bedding directions at 1 MHz frequency was performed by establishing an experimental system for resistivity testing of coal under triaxial stress. The low-pressure nitrogen gas adsorption (LP-N_2GA) experiment and scanning electron microscopy (SEM) were obtained to analyze the pore-fracture structural characteristics of coal samples and the influence on resistivity anisotropy. Furthermore, the fundamental cause of anisotropy of coal resistivity is expounded systematically. The results show that the resistivity of loaded coal decreased first before increasing. The ionic conductance and the high degree of metamorphism slow down the decrease of resistivity. The distribution of pore and fracture structures is anisotropic. The connected pores and fractures are mainly distributed along the parallel bedding direction. The weak plane of bedding, diagenetic fractures, and plane fracture structures of parallel bedding result in the increase of fractures in the direction of vertical bedding, so increasing the potential barrier. Therefore, the resistivity in the vertical bedding direction is higher than that of the parallel bedding. Loading coal resistivity anisotropy degree is a dynamic change trend; the load increases anisotropy significantly under axial pressure, and the degree of anisotropy has a higher discreteness under confining pressure. It is mainly the randomness of the internal pore-fracture compaction, closure, and development of the heterogeneous coal under the confining pressure; the more rapid the decline in this stage, the larger the stress damage degree.

1. Introduction

In recent years, China's demand for coal energy keeps increasing, which leads to the stage of deep mining. The increase of mining depth and intensity increases the possibility of coal-rock composite dynamic disasters such as rock burst and coal and gas outburst [1, 2]. Research on electrical parameter changes based on the electrical and physical properties of coal is the physical property prerequisite for conducting electrical exploration in underground coal mines [3, 4]. Dynamic prediction without damage based on resistivity testing principle plays a positive role in monitoring and forecasting coal and rock dynamic disasters.

The development of cracks is also synchronized with the advancement of the working face, and there are vertical subsidence and horizontal deformation of the rock strata [5]. The response position of abnormal high resistance of loaded coal is consistent with the fracture development position [6]. By monitoring the local resistivity and its anisotropy change, the coal and gas outburst can be predicted and forewarned [7]. Therefore, scholars at home and abroad have studied the resistivity change characteristics of loaded coal. Different pore size, distribution, and connectivity lead to distinct resistivity, and pore structure has a significant effect on resistivity [8]. The change of electrical parameters of loaded coal is obviously consistent with the stress. The electrical parameters can better reflect the formation, development, and penetration of microfracture, as well as the characteristics of changes in the internal structure in the failure process of coal and rock [9, 10]. The direction of the anisotropic principal axis of the rock with the largest change in the apparent resistivity is basically the same as the direction of the main fracture of the rock. There are significant anisotropy of measured points in cracks and fractured zones

[11, 12]. Xu et al. [13] explored the anisotropy change of rock under uniaxial compression by defining the anisotropy factor, which proposed that the anisotropy change tends to rise at the first macrofracture time. Chen et al. [14] put forward the concept of series-parallel dominance and analyzed the law that the resistivity of anthracite increases at different temperatures as the sampling angle increases. An anisotropic multilayer model was established by Shen to analyze the apparent resistivity of anisotropic formation. It was found that the apparent resistivity of the perpendicular formation is greater than that of the parallel formation [15]. The permeability of parallel bedding sample is higher than that in the vertical bedding sample [16]. The permeability of coal is highly anisotropic even on a small scale, which is controlled by cleat properties [17]. Liu et al. [18] found that the dispersion degree of tensile strength in the vertical bedding direction of coal is smaller than that in the parallel bedding direction, and the anisotropy of mechanical properties is affected by the strip distribution of macrocoal components and the directionality of the distribution of cleat system. Uniaxial compressive strength of parallel and vertical bedding coal samples is different, which is controlled by bedding structure [19]. Therefore, bedding and pore-fracture structure may also be the key to affecting the anisotropy of resistivity.

Previous studies have focused on the various characteristics and anisotropy of coal resistivity in different bedding directions under uniaxial compression. The influence of pore-fracture structure characteristics, charge transfer, and loading path on resistivity anisotropy remains to be further analyzed. It is necessary to comprehensively and systematically understand the influence of coal and rock bedding on resistivity anisotropy characteristics. Therefore, an experimental system for resistivity testing of coal under triaxial stress is established. The change laws and mechanisms of resistivity anisotropy under different loading paths are analyzed by experimental and theoretical research to provide a certain theoretical basis for the prediction of coal and rock dynamic disasters.

2. Experimental System and Method

2.1. Experimental System. As shown in Figure 1, the system is composed of a three-axis pressurization device, a resistivity measuring device, a temperature control device, and a computer for data collection. The following briefly introduces the structure and function of each device. The three-axis pressurization device is designed by the laboratory to realize the axial and confining pressure loading of the elastic cavity through water pressure. The pressure control range is 0–16 Mpa and measurement control accuracy is 0.01 Mpa. Resistivity test device uses HIOKI 3532-50 LCR tester instrument connected to PC and then collects data continuously in its software. It can display parameters such as impedance, phase angle, inductance, capacitance, and resistance at the range of 5 MHz. The temperature control device employs ES-III temperature controller manufactured by Changzhou Easy-to-Use Technology Company to achieve constant temperature control of the coal samples.

2.2. Samples and Method. The coal samples were from Dashucun, Sihe, Yuwu Coal Mine in Shanxi province in China. Large coal samples with good integrity were processed into a Ø25 mm × 50 mm cylinder. The core sampling direction of the drilling sampler is vertical or parallel to the coal bedding direction, and test specimens with different bedding directions are drilled in the same coal sample. Ensure that the stress of the coal samples is uniform to prevent the damage of the coal body caused by the stress concentration, reduce the visible cracks as much as possible, and timely mark sample with different bedding directions. In order to eliminate errors caused by sample irregularities and the test electrode well coupled with specimens, the surface of samples is smooth and cylindrical end face evenness error is less than 0.02 mm. Finally, complete, dense, and no obvious crack test specimens were selected, as shown in Figure 2. It should be noted that the vertical bedding refers to the axis of the sample being perpendicular to the bedding plane, and the parallel bedding refers to the axis being parallel to the bedding plane.

The experimental procedures are as follows:

(1) Industrial analysis, low-pressure nitrogen gas adsorption (LP-N_2GA), and scanning electron microscopy (SEM) tests were carried out on Dashucun, Sihe, and Yuwu coal samples to study and analyze the microstructure of coal.

(2) The cored coal samples were placed in the electrical parameter test chamber, the copper electrode and the end face were coupled with conductive glue, and enameled wire was connected with the LCR tester. Before loading in different paths, a certain preload was applied to fix the specimen in the elastic cavity, and the coal samples with different bedding directions were increased the axial pressure to 9 Mpa step by step, and the computer recorded the change of electrical parameters of the loaded coal sample. After the axial loading was completed, the above steps were repeated, and the confining pressure of coal samples with different bedding directions gradually increased to 8 Mpa.

According to the working principle of LCR tester, the resistivity calculation formula is as follows:

$$|Z|\cos\theta = R,$$
$$\rho = |Z|\cos\theta\frac{S}{L} = R\frac{S}{L}, \quad (1)$$

where Z is the impedance absolute (Ω); θ is the phase angle (°); ρ is the resistivity (Ω·m); R is the resistance (Ω); S is the sample cross-sectional area (m^2); and L is the sample length (m).

In order to facilitate the analysis of experimental results, SDLA618 industrial analyzer was used to measure the basic parameters of coal samples in different mining areas according to GB/T212-2008 Industrial Analysis of Coal. V_{daf} is used to quantify the degree of coal metamorphism. The

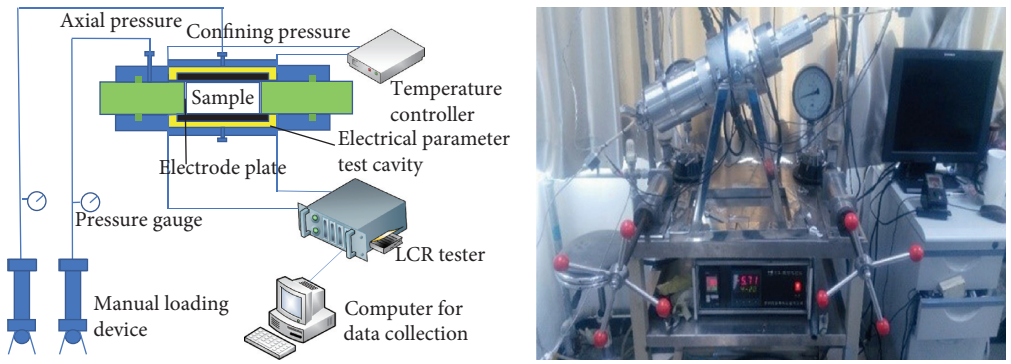

Figure 1: Diagram of loaded coal resistivity test system. (a) Schematic diagram. (b) Physical diagram.

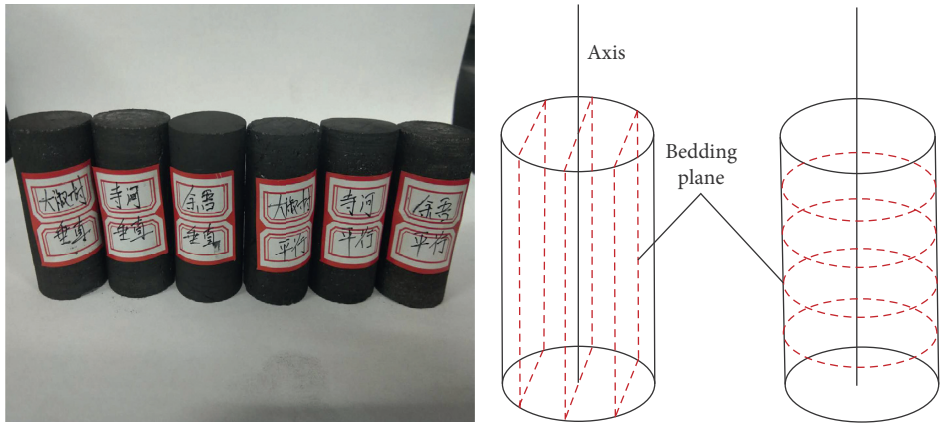

Figure 2: Parallel and vertical bedding direction coal samples. (a) Experimental coal samples. (b) The bedding direction.

higher the degree of metamorphism, the smaller the V_{daf}, and the results are shown in Table 1.

3. Experimental Results on Resistivity Anisotropy of Loaded Coal Samples

The variation of the resistivity of coal samples with different bedding direction was measured under axial pressure and confining pressure during 1 MHz frequency. The temperature of the coal samples was controlled at 30°C to reduce the interference of temperature on resistivity changes.

According to the experimental results of specimens with different bedding directions, the change curves of coal samples resistivity under different axial pressure and different confining pressure were drawn, as shown in Figures 3(a)–3(f). Under the axial pressure process, the resistivity of coal samples in different mining areas does not have to vary synchronism as stress increases. The change of coal samples resistivity in Dashucun is characterized by "rapid decline-gentle rise-rapid decline." Sihe is characterized by "slow decline-rapid decline-sudden increase," and is irregular "V" shape [20, 21]. Yuwu is characterized by "serrated fluctuations-abruptly decreased." There are

Table 1: Industrial analysis basic parameter.

Samples number	Coal rank	M_{ad}	V_{daf}	A_d	FC_{ad}
DSC	Lignite	0.45	51.18	2.65	45.72
SH	Lean coal	1.92	7.39	13.36	77.33
YW	Lean coal	2.38	4.79	14.59	78.24

obvious differences in the resistivity changes of coal samples in different mining areas under axial pressure. There is no inflection point of resistivity sudden increase in Dashucun and Yuwu coal samples during the loading process. It is considered that the data recording is incomplete and the stress has not reached the value of expanding the coal body, which was related to the pore structure and sedimentation metamorphism of the coal body. Under confining pressure, the resistivity of coal samples in different bedding directions has obvious consistency as stress increases. The resistivity decreases rapidly at the beginning and the rate of decline decreases gradually. After the confining pressure increases to a certain value, the resistivity starts to fluctuate and rise.

Although the range of resistivity measured in experiments is large, it can be seen from Figure 3 that the resistivities of different bedding directions in all coal samples are

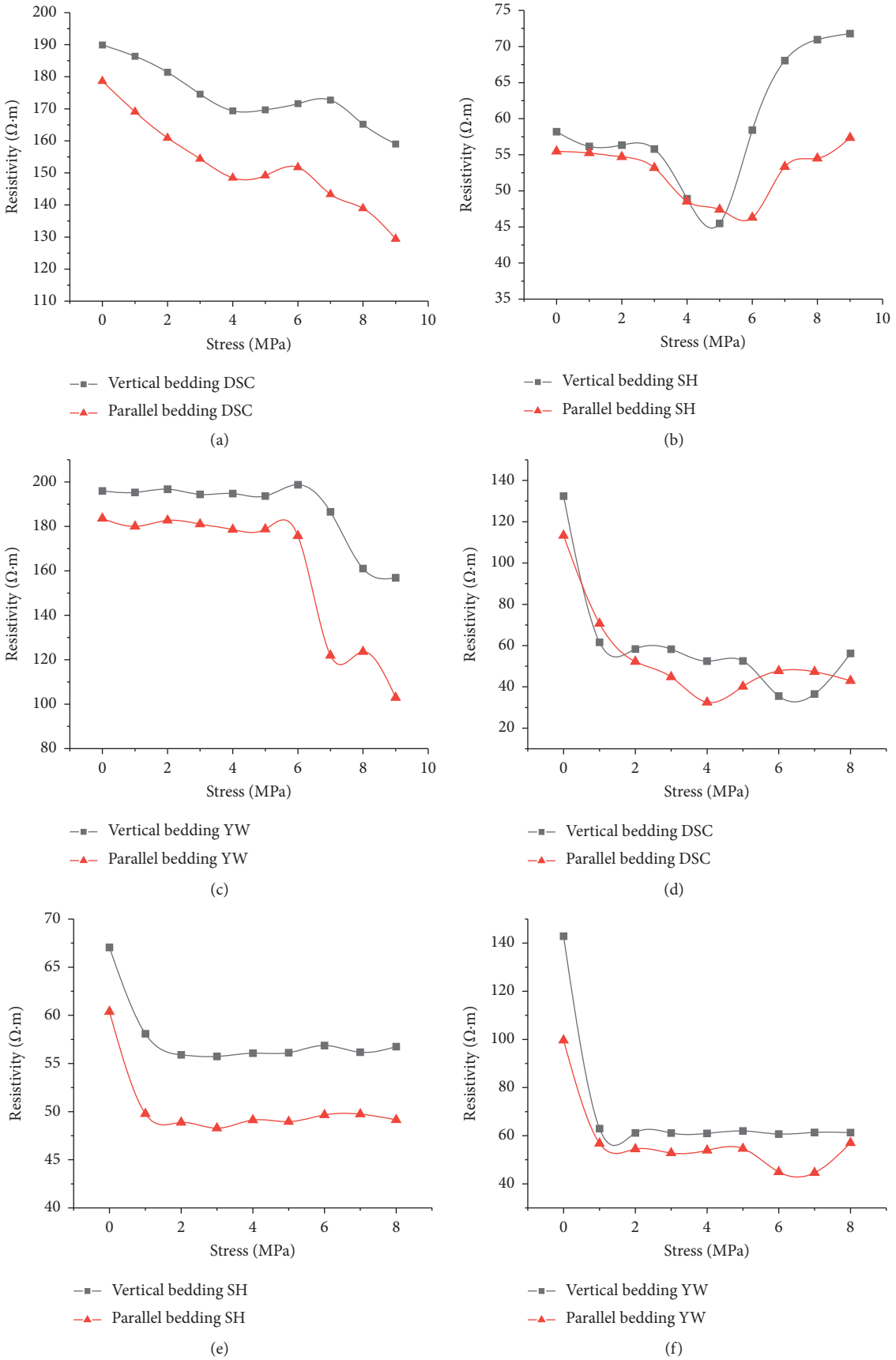

Figure 3: Resistivity curves in different bedding directions. (a) Dashucun coal samples under axial pressure. (b) Sihe coal samples under axial pressure. (c) Yuwu coal samples under axial pressure. (d) Dashucun coal samples under confining pressure. (e) Sihe coal samples under confining pressure. (f) Yuwu coal samples under confining pressure.

not equal. The resistivity of coal has obvious anisotropic characteristics. The resistivity in the vertical bedding direction is greater than that in the parallel bedding. Coal is highly anisotropic and heterogeneous [17, 22], affecting coal resistivity. The high degree of coal heterogeneity results from a combination of many geological factors including sediment sources, depositional environments, tectonic settings, diagenesis, climate, and hydrological conditions [23, 24]. The heterogeneity of coal increases the uncertainty of the development and connection of the pores and cracks of the loaded coal. Therefore, the resistivity in the parallel bedding of singular points is greater than that of the vertical bedding. The variation curves of coal resistivity of different bedding directions under the same loading path are similar. Therefore, it is considered that the bedding structure has no impact on the total variation characteristics of the resistivity. Resistivity first decreases and then increases during coal samples loading, and the resistivity can better respond to the relationship between load and pore-fracture. The change of bulk structure is still the determinant of resistivity change during the loading process; pore-fracture deformation, crack initiation, and propagation are the main factors.

4. Discussion and Analysis

4.1. Effect of Pore and Fracture Structure and Its Anisotropy on Resistivity. The coal metamorphism degree and pore structure are different in different geological areas. Through LP-N_2GA and SEM of coal samples, the characteristics of pore-fracture structure and its influence on coal resistivity anisotropy were investigated. Smashing and screening coal samples with a particle size of 60–80 mesh were carried out for vacuum degassing, conducting low-temperature nitrogen gas adsorption. When the relative pressure of condensation and evaporation of a pore is different, the so-called adsorption loop is formed, LP-N_2GA isotherms as shown in Figure 4.

Based on the experimental data of low-temperature nitrogen gas adsorption of coal samples, the specific surface area of coal samples was calculated according to the BET multilayer adsorption theory, and the pore size distribution was calculated by BJH model, as shown in Table 2.

If the pore structure is different, the adsorption capacity is different. The adsorption loop reflects the distribution of different pore structure of coal samples in different mining areas [22, 25], so as to understand the pore structure type of coal. Dashucun coal samples showed capillary condensation at a relative pressure of 0.5 MPa, which demonstrates that the pore morphology is relatively simple. There are open cylindrical pores and bottle-shaped pores, whose connectivity is general. Sihe coal samples adsorbed the least N_2 at the highest pressure and the adsorption/desorption isotherms are relatively close, which illustrates the limitation of pores number and poor porosity. The nonconnected cylindrical pores and the slit-shaped pores account for the majority, and the pores with poor connectivity are dominant. The pore structure of Yuwu coal is complex, the connectivity in the pore is very good, and the micropore clusters are developed, so the adsorption capacity is strong and the hysteresis loop is highly separated. SEM can directly visualize the micro-nanoscale solid surface micromorphology and analyze the pore structure of coal with different metamorphic degrees through the development characteristics of pore, as shown in Figure 5. The deep part of the image represents pores, while the shallow part is nonpores. Under the same magnification ratio, the microsurface morphology of coal with different metamorphism degrees is obviously different. Under the SEM 5000 times magnification, the surface of the Dashucun coal is rough with many pores and fractures, the surface of Sihe is flat with rare fractures, the surface of Yuwu has many pores and microfractures, and the original structure of the coal body is clear. Besides, the microstructure of the coal samples under SEM is consistent with the experimental results of LP-N_2GA.

The pore size of Dashucun is dominated by macropores, which above 50 nm [26] is 51.63%, and the proportion of mesopore is 23.09%. The macropores and mesopores account for more than 70% of the pore structure; the conductivity is poor with low compactness and development pore-fracture, so the resistivity value before loading is large [27]. With the deepening of the degree of metamorphism, the polycondensation of coal macromolecular structure is increased and tends to be ordered [28]. The total pore volume of Sihe is the smallest, the compactness is high, and the conductivity is strong. The Yuwu coal samples have large porosity and well connectivity, microcracks develop obviously, and the conductive channel is destroyed to a certain extent, so the resistivity before loading is large. The response law of acoustic emission parameters of loaded coal can be divided into the initial loading stage, the slow increase stage, the sharp increase stage, and the damage instability stage [29]. The response law of resistivity is also divided into four stages: densification stage, elastic stage, plastic stage, and breakage stage [30]. At the early stage of loading, the microcracks and pores of the coal body are compressed and closed, the contact between the particles inside the coal body is tighter, the conductive channel gets better, the electrical conductivity increased, and resistivity shows descending tendency. With the loading of pressure, pores and cracks have been almost completely enclosed to the elastic stage. The interaction between the intermolecular electron clouds in the compact coal body is remarkable, the electron mobility increases, and the resistivity further descends [31]. With the occurrence of the inflection point of coal resistivity with dilatation, microfracture has occupied a dominant position; the conductive channel suffers from breakage and then causes resistivity to rise. Finally, when the pore fracture develops into a large fracture zone, the conductive channel is severely damaged, and the resistivity is far higher than the initial value.

Coal is a complex porous medium composed of pores, fissures, and coal skeletons; the degree of pores and fractures development in different directions is not the same under the action of sedimentation and geological structure. Cleats are fractures that are mutually perpendicular and also perpendicular to bedding, which are confined to individual coal beds. Vertical connectivity of cleat networks is commonly limited by the termination of small cleats at interfaces

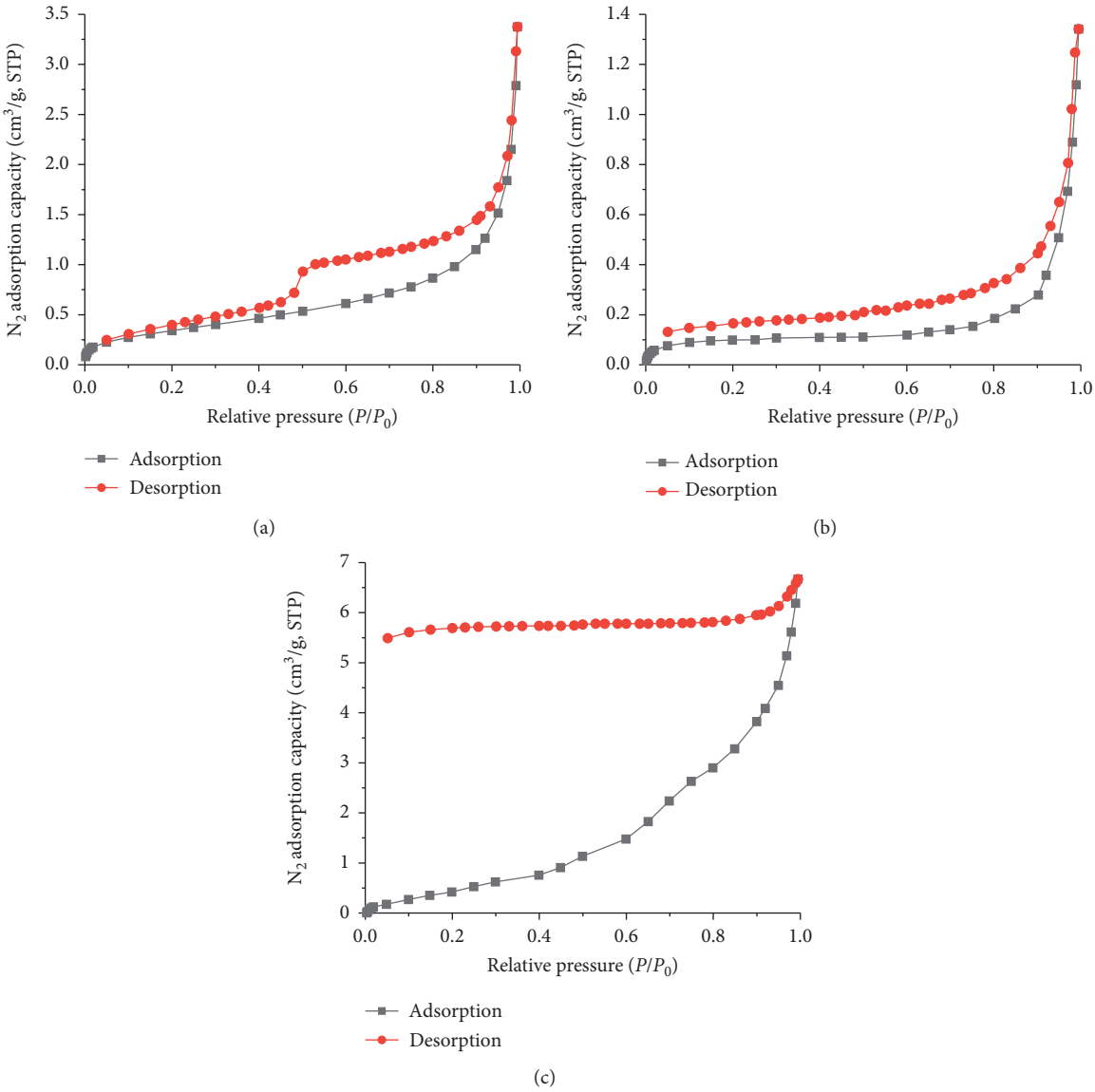

Figure 4: LP-N_2GA isotherms for three coal samples. (a) Dashucun. (b) Sihe. (c) Yuwu.

Table 2: Microscopic parameters of coal samples.

Sampling sites	Total pore volume ($cm^3 \cdot g^{-1}$)	Pore size distribution			Specific surface area ($m^2 \cdot g^{-1}$)	Porosity (%)
		Micro (<2 nm)	Meso (2~50 nm)	Macro (>50 nm)		
DSC	0.002153	25.28	23.09	51.63	1.188	9.3
SH	0.001735	55.35	24.31	20.34	0.375	6.1
YW	0.002510	69.89	15.14	13.96	1.165	8.2

between coal types, so connectivity is poor in vertical bedding direction [32]. Based on the nuclear magnetic resonance (NMR) method, it was found that the pores of parallel bedding coal samples were tightly closed after uniaxial compression, some of the fractures were deformed radially, and the crack closure effect in the vertical bedding direction was significant [33]. Fissures in the coal body are the main channels for gas flow, and the permeability is large in the direction of parallel bedding. The connected pores and fractures are mainly distributed along the bedding direction, the pores and fractures in the vertical bedding direction are poorly connected, and the tortuosity of the seepage channel is large [34, 35]. Previous studies showed that the calcite particles uniformly distribute on the bedding planes [19, 24], and a large number of pores almost parallel to the bedding are formed on the edges of the minerals due to compaction

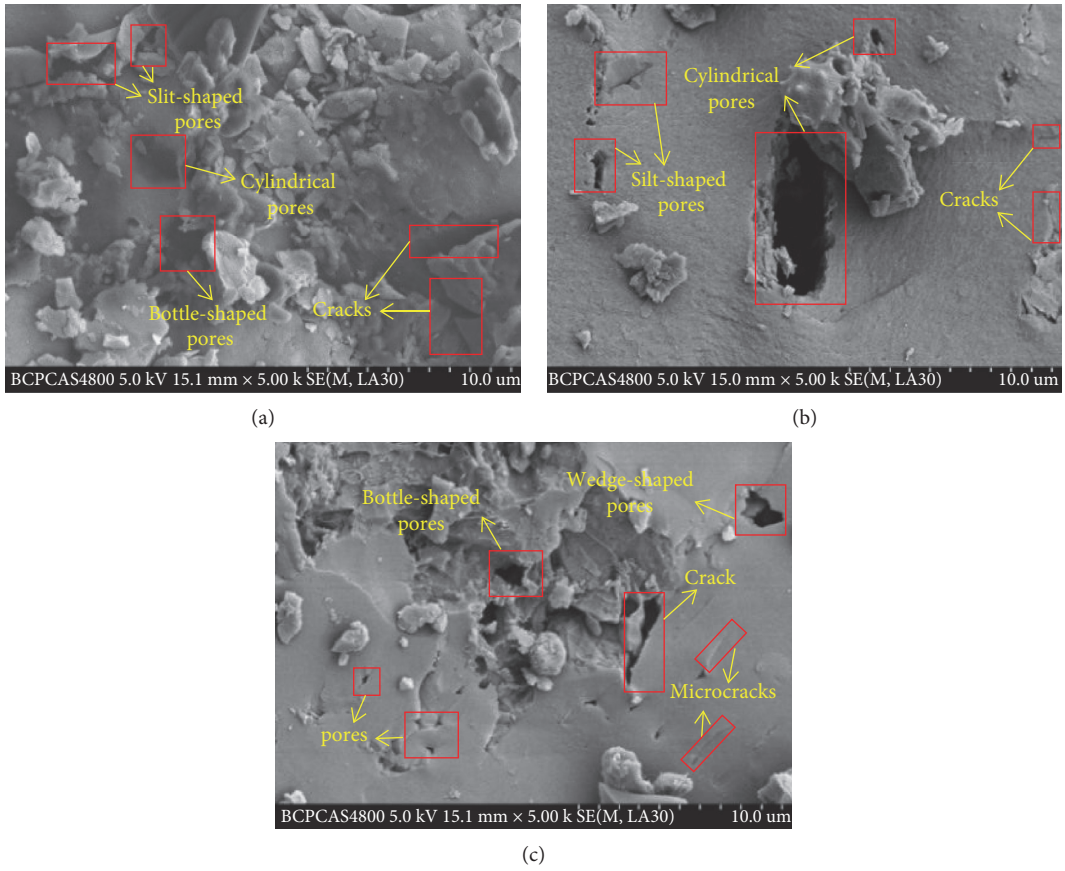

Figure 5: The SEM image at 5000 magnification. (a) Dashucun. (b) Sihe. (c) Yuwu.

by sedimentation. The bedding fractures can be formed during diagenesis. In addition, the fractal theory is applied to the study of coal fracture development and distribution. The fractal box dimension can be used to characterize the development degree of coal fracture. It was found that the fractal box dimension of parallel bedding direction fracture is larger than that of vertical bedding [36]. The surface fissure structure of the parallel bedding is developed, and the distribution of the fissures shows a certain dominant orientation [16, 37]. In summary, there are anisotropic features in the pore-fracture structure distribution in different bedding directions. The pores and fractures develop along the bedding direction, and the structure parallel to bedding has well connectivity. Bedding planes and fissure channels are the dominant channel for gas migration, as shown in Figure 6. The distribution characteristics of pores and fractures make the charge transfer difficult to be different. Migration along the direction of bedding is easy to the vertical bedding. Therefore, the resistivity in the vertical bedding direction is higher than that of the parallel bedding.

4.2. Effect of Charge Transfer on Resistivity Anisotropy. One of the important characteristics of coal as a sedimentary rock is the existence of bedding structure. The difference of vertical bedding direction resistivity and parallel bedding resistivity is one of the concrete manifestations of resistivity anisotropy. The difference in conductivity of coal samples with different bedding directions under load conditions is obvious. The conductivity of the vertical bedding sample is lower than that of the parallel bedding. The resistivity of the loaded sample is 68.6 Ω·m higher than that of the parallel bedding sample.

The anisotropic characteristics of resistivity can be analyzed from both microscopic and macroscopic aspects. Microscopically, electrons must overcome coal molecules barrier from one atom to another. Coal is a macromolecular structural unit composed of an aromatic ring as a core; when electrons move in an aromatic layer, the barrier mainly refers to the binding of large molecules of coal to electrons, but when electrons move between the aroma layers, the electrons not only have to overcome the binding force of the coal macromolecules to electrons, but also overcome the force of the electrons penetrating the aromatic parallel stack. The structural characteristics of the weak plane of the bedding make it difficult for carriers to move between the bedding, and there is a barrier to the bedding. The total barrier in the direction of parallel bedding is mainly the standard barrier, while vertical bedding direction is composed of the standard barrier, penetrating the potential barrier and bedding barrier. It is difficult for electrons to migrate in a parallel bedding than vertical bedding, so the conductivity in the parallel bedding direction is higher [38]. In a macroscopic view, the plane of bedding has a weak cementation degree.

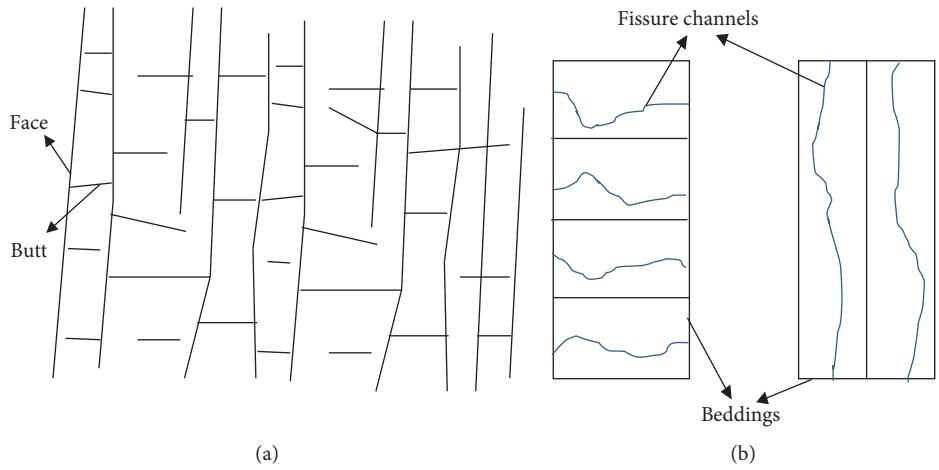

Figure 6: Schematic diagram of fracture distribution. (a) Cleat-trace patterns in plan view. (b) Distribution of fissure channel.

Micro and medium fractures are relatively developed under the combined action of internal and external stress [39]. The contact between bedding is not dense under the same bedding and usually has different dielectric constant and conductivity. The anisotropy of pores and fractures distribution makes the connected pores and fractures develop into dominant channels along the bedding direction, and the total fissure degree of vertical bedding sample is greater than that of parallel bedding [16]. The migration of charge between the bedding plane and the fracture channel will be hindered. In the parallel bedding, the fracture zone that the charge needs to pass through is relatively reduced, and the electrical conductivity is high. Also, the free charge tends to move along the bedding column under the external electric field and continues to move toward the lower potential end when it is in equilibrium. The current density on different bedding columns is different. When the charge accumulates on the bedding plane, a new electric field E' is formed, which hinders the movement of the charge to the low potential direction, and the sample resistivity increases [15], as shown in Figure 7. The distribution of the bedding plane and the fracture structures makes the resistivity of the vertical bedding equivalent to the series connection of multiple resistances. The resistivity of the parallel bedding is similar to the parallel connection. Therefore, The bedding resistivity has obvious anisotropy characteristics.

4.3. Effect of Loading Path on Resistivity Anisotropy. It can be seen from Figure 3 that the change law of resistivity of loaded coal samples under different loading paths. The changing trend of resistivity under different loading paths is different; the rate of resistivity decrease under confining pressure is greater than axial pressure at the initial loading. It is considered to be related to the variation of the loaded fracture and the large pore size under different loading paths. Based on the bending deformation theory of simple support, the deformation of pore and fracture under confining pressure loading was discussed [40]. The effect of stress on pores and fractures strain is different. The fracture is higher than macropores, mesopores, and micropores; the larger the fracture width and the larger the pores, the higher the deformation degree. At the beginning of confining pressure loading, fracture and macropores are closed rapidly, the conductive channel increases, and the resistivity decreases rapidly. The influence of confining pressure on micropores is limited, resistivity reduction tends to flatten out after 2 Mpa, and the resistivity tends to increase with the expansion, development, and transfixion of microcracks. Compared with axial pressure, the confining pressure has a better compaction effect on the pore-fracture structure [41], and the deformation in the early stage is the largest. The sample has a stronger sensitivity to confining pressure, the pore-fracture closure rate is faster after loading, and the sample is also the most damaged.

The anisotropy coefficient is defined as follows:

$$\lambda = \sqrt{\frac{\rho_n}{\rho_t}}, \tag{2}$$

where ρ_n is vertical bedding direction resistivity and ρ_t is parallel bedding direction resistivity.

The closer the anisotropic coefficient λ value is to 1, the lower the resistivity anisotropy characteristic appears, and the more the deviation from 1 is, the more obvious the anisotropic characteristic is. Calculate the anisotropy coefficient and the degree of deviation of the resistivity anisotropy coefficient during the loading process, as shown in Figure 8.

The λ deviation value reflects the degree of resistivity anisotropy of coal rock. It can be seen from Figure 8 that the resistivity anisotropy is obvious during the loading process. There are obvious dispersions of the λ deviation values under different loading paths, but the dispersion degree is higher under confining pressure. When the stress increases during axial pressure, the λ deviation value of coal samples in different mining areas changes significantly. As the stress increases, the degree of anisotropy increases. The dispersion of λ deviation under confining pressure loading is heavy, and axial pressure has a better influence on resistivity anisotropy than confining pressure. Affected by the heterogeneity and

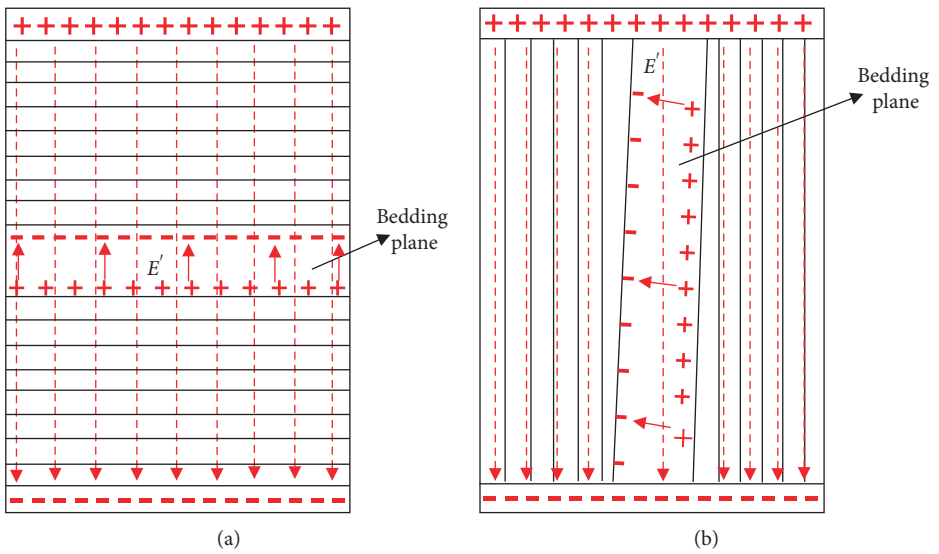

Figure 7: Schematic diagram current conduction. (a) Vertical bedding. (b) Parallel bedding.

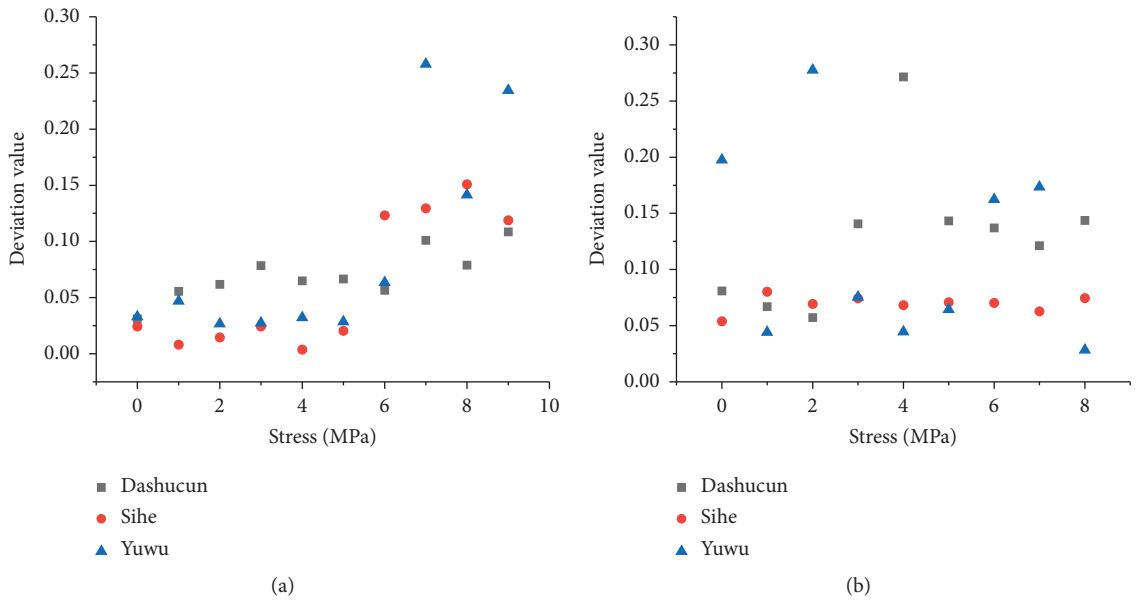

Figure 8: λ deviation degree under different loading paths. (a) Axial pressure. (b) Confining pressure.

the direction of confining pressure, the compaction, development, and transfixion of the pore-fracture are random and uneven, so anisotropic sudden increase or sudden decrease occurs during loading, and the variation law is not clear. It is not hard to find that the degree of anisotropy of the resistivity of the loaded coal is dynamically changing. The development of coal pore-fracture is the main factor in the change of resistivity anisotropy. The overall feature is that the resistivity anisotropy is significant with the stress increases under axial pressure.

4.4. Influence of Mineral Elements on Electrical Resistivity. According to the solid dielectric theory [42], solid conductivity is divided into ionic conductivity (intrinsic conductivity and impurity conductivity) and electronic conductivity. The intrinsic conductivity is affected by the thermal movement of ions in the crystal lattice, so the ionic conductivity is dominant at room temperature. The general expression of conductivity is

$$\sigma = \sum \sigma_i = \sum_i n_i e_i \mu_i, \tag{3}$$

Table 3: EDS element analysis table.

Coal sample	Element	Mass percentage	Atomic percentage
DSC	Al	3.654	1.829
	Si	3.128	1.519
	Ga	0.364	0.121
SH	Al	3.458	1.734
	Si	3.690	1.840
	Ga	1.020	0.382
	Fe	0.262	0.061
YW	Al	2.879	1.441
	Si	3.863	1.926
	Ga	1.829	0.611
	Fe	9.102	2.118
	Na	0.632	0.321
	Cl	0.501	0.210

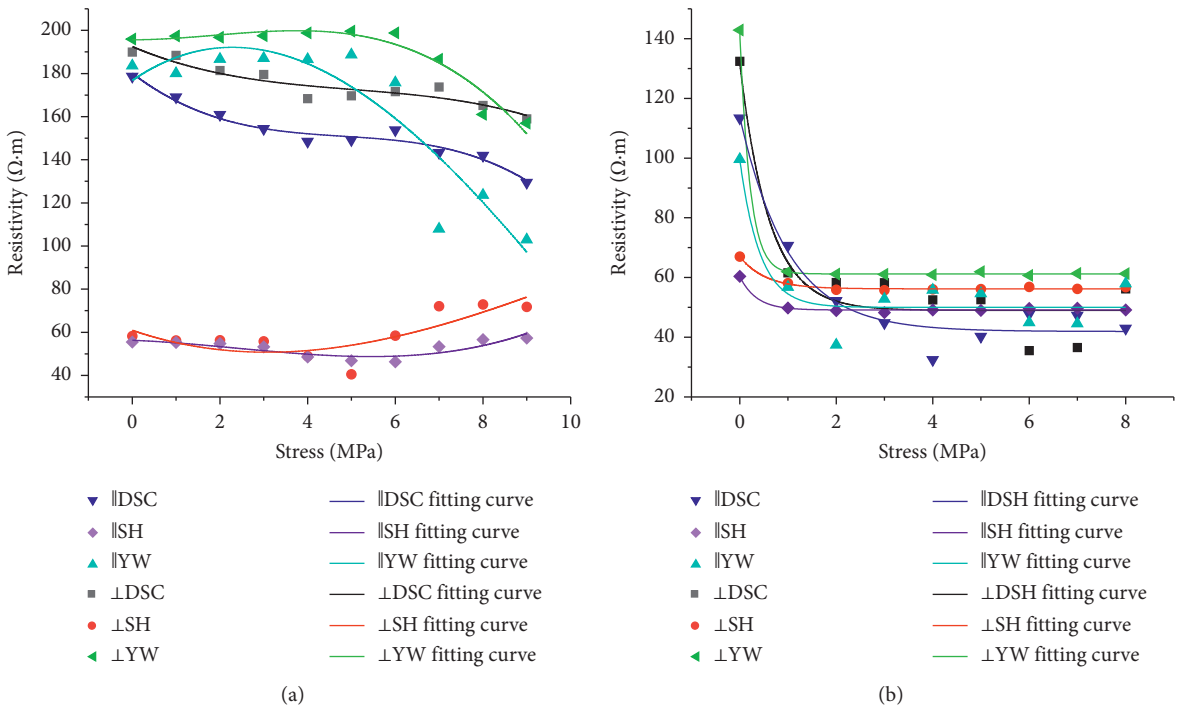

Figure 9: Resistivity fitting curve under stress. (a) Axial pressure. (b) Confining pressure.

where σ is conductivity; n_i is carrier concentration; e_i is charger charge; and μ_i is carrier mobility.

The conductance mechanism of coal when loaded is also ionic conductivity and electronic conductivity [9, 21]. It is found from Figure 3 that the resistivity of Sihe and Yuwu coal samples under axial pressure did not decrease significantly with the increase of stress, which is considered as the result of the interaction between ionic conductivity characteristics and compact coal structure. The mineral elements of coal samples from different mining areas were analyzed by EDS spectrometer, as shown in Table 3.

Dashucun coal samples are rich in macropores, mesopores, and fissures; the internal moisture and mineral elements are scarce, so the electronic conductivity is absolutely dominant during the process of axial pressure; coal resistivity decreases rapidly after loading. The metamorphic degree, intrinsic moisture, and mineral elements of other coal samples are higher. Under stress loading, coal particle pores and cracks are closed, the intermolecular distance on the microscopic level is also reduced, the free space available for ion transition is reduced, the ion mobility is reduced, and the ion conductivity is reduced, resulting in an increase in resistivity [43]. At the same time, the close contact between the coal particles facilitates the circulation of electrons; the electronic conductivity is enhanced and the resistivity is decreased. Therefore, the initial resistivity of the loaded coal is slowly decreased and fluctuated, and there is no significant drop and rise. The bedding plane is mixed with different mineral compositions. These channels change the electrical properties of the coal body, and the interlayer channels

weaken the migration barrier of ion carriers [44]. The distribution of mineral elements on coal samples in vertical and parallel bedding has a positive effect on electrical conductivity.

4.5. Influence of Anisotropy on Stress-Resistivity Relationship. When the temperature is constant and the coal body is under pressure, the formula [31] for expressing the conductivity can be described as follows:

$$\gamma = A \exp(B\sigma), \tag{4}$$

where γ is the resistivity, σ is stress, and A and B are the coefficients.

By fitting the original data, it is found that the resistivity of coal fitting relation of axial pressure and confining pressure is different, as shown in Figure 9. The relationship under the axial pressure fitting is as shown in (5), and the fitting relationship under the confining pressure is as shown in (6):

$$y = y_0 + b_1 x + b_2 x^2 + b_3 x^3, \tag{5}$$

$$y = A \exp(R_0 x) + R_1, \tag{6}$$

where x is stress; y is the resistivity; and b_1, b_2, b_3, A, R_0, and R_1 are the coefficients associated with coal.

It is consulted by the fitting relationship under different loading paths that the loading paths have a significant influence on the stress-resistivity relationship. The correlation of the cubic polynomial fitting under axial pressure is higher, and the fitting degree of the formula (6) under confining pressure loading as well (R^2 is much larger than 80%) is good. Coal is highly anisotropic and heterogeneous, bedding structure is one of its important characteristics, and the distribution of pore-fracture also has anisotropic characteristics. Samples in different regions have a high degree of heterogeneity, and the pore-fracture structure of the samples is completely different under the microcosm, so there are no synchronization of resistivity changes under loading. For coal samples with different bedding directions, there is an anisotropy in pore-fracture structure distribution, but the degree of coal metamorphism and pore development are the same. The experiment and fitting results show that the anisotropy has basically no effect on the changing trend of the resistivity of the loaded coal samples under the same loading path. The resistivity of coal samples with different bedding directions has the same trend with stress, and the resistivity in the vertical bedding direction is greater than that in the parallel bedding.

5. Conclusions

Based on previous studies, the microstructure, loading path, resistivity change, and anisotropy of coal samples with different bedding directions were experimentally studied, and the following conclusions were obtained:

Coal is highly heterogeneous and anisotropic. The pore structure of coal with different metamorphisms varies greatly. The distribution of pore and fracture structure is anisotropic. The connected pores and fractures are mainly distributed along the parallel bedding direction; the pores and fractures in the vertical bedding direction are poorly connected. Compressive deformation, crack initiation, propagation, and coalescence of coal samples lead to resistivity undergoing the process of descending-to-ascending trend. Macropore, mesopore, and fracture development of coal samples make the resistivity even larger.

There are anisotropic characteristics of coal resistivity. The weak plane of bedding, diagenetic fractures, and plane fracture structures of parallel bedding result in the increased of fissures degree in the direction of vertical bedding. The vertical bedding direction has a large total potential barrier, which electron migration is difficult. The resistivity of coal samples in the direction of vertical bedding is larger than that of parallel bedding.

The resistivity change of loaded coal under axial pressure and confining pressure have significant difference, the pore fracture is quickly closed at the beginning of confining pressure loading, so the degree of stress damage is the largest. The anisotropy factor is introduced to explore the response characteristics of resistivity anisotropy in the failure process of the samples and find its dynamic change trend. On the whole, the degree of resistivity anisotropy increases with stress under axial pressure; the anisotropy dispersion is higher under confining pressure.

Data Availability

All data used to support the study are present in the article as figures or tables.

Conflicts of Interest

The authors declare that they have no conflicts of interest regarding the publication of this paper.

Acknowledgments

This study was supported by the Natural Science Foundation of Beijing Municipality (Grant no. 8192036), the National Key Research and Development Program of China (Grant no. 2018YFC0808301), Youth Foundation of Social Science and Humanity, the Ministry of Education of China (Grant no. 19YJCZH087), the State Key Laboratory Cultivation Base for Gas Geology and Gas Control (Henan Polytechnic University) (Grant no.WS2018B04), and the Fundamental Research Foundation for the Central Universities (Grant no. 2009QZ09).

References

[1] X. Kong, E. Wang, S. Hu, R. Shen, X. Li, and T. Zhan, "Fractal characteristics and acoustic emission of coal containing methane in triaxial compression failure," *Journal of Applied Geophysics*, vol. 124, no. 1, pp. 139–147, 2016.

[2] G. Cheng, T. Ma, C. Tang, H. Liu, and S. Wang, "A zoning model for coal mining-induced strata movement based on microseismic monitoring," *International Journal of Rock*

Mechanics and Mining Sciences, vol. 94, no. 4, pp. 123–138, 2017.

[3] N. Bai-Sheng, H. Xue-Qiu, and Z. Chen-Wei, "Study on mechanical property and electromagnetic emission during the fracture process of combined coal-rock," *Procedia Earth and Planetary Science*, vol. 1, no. 1, pp. 281–287, 2009.

[4] J. E. Chambers, P. B. Wilkinson, A. L. Weller, P. I. Meldrum, R. D. Ogilvy, and S. Caunt, "Mineshaft imaging using surface and crosshole 3D electrical resistivity tomography: a case history from the East Pennine Coalfield, UK," *Journal of Applied Geophysics*, vol. 62, no. 4, pp. 324–337, 2007.

[5] X. Yang, G. Wen, L. Dai, H. Sun, and X. Li, "Ground subsidence and surface cracks evolution from shallow-buried close-distance multi-seam mining: a case study in bulianta coal mine," *Rock Mechanics and Rock Engineering*, vol. 52, no. 8, pp. 2835–2852, 2019.

[6] T. Zhu, J. Zhou, and J. Hao, "Resistivity anisotropy and its application in earthquake research," *Progress in Geophysics*, vol. 24, no. 3, pp. 871–878, 2009.

[7] H. Lu and Y. Jia, "Experimental study on change law of restivity of coal under compressive load," *Mining Research and Development*, vol. 29, no. 4, pp. 36-37, 2009.

[8] L. Sima, D. Huang, S. Han et al., "Effectiveness evaluation of palaeo-weathering crust-type karst reservoirs in the Southern Jingbian Gasfield, Ordos Basin," *Natural Gas Industry*, vol. 35, no. 4, pp. 7–15, 2015.

[9] W. Yungang, W. Jianping, and Y. Song, "Experimental research on electrical parameters variation of loaded coal," *Procedia Engineering*, vol. 26, pp. 890–897, 2011.

[10] L. Qiu, D. Song, E. Wang et al., "Determination of hydraulic flushing impact range by DC resistivity test method," *International Journal of Rock Mechanics and Mining Sciences*, vol. 107, pp. 127–135, 2018.

[11] F. Chen, J. An, and C. Liao, "Directionality of resistivity change of anisotropy rock with original resistivity," *Chinese Journal of Geophysics*, vol. 46, no. 2, pp. 381–395, 2003.

[12] D. Song, Z. Liu, E. Wang, L. Qiu, Q. Gao, and Z. Xu, "Evaluation of coal seam hydraulic fracturing using the direct current method," *International Journal of Rock Mechanics and Mining Sciences*, vol. 78, pp. 230–239, 2015.

[13] X. Xu, B. Liu, S. Li et al., "Experimental study on conductivity anisotropy of limestone considering the bedding directional effect in the whole process of uniaxial compression," *Materials*, vol. 9, no. 3, p. 165, 2016.

[14] L. Chen, Y. Zhang, Z. Huang et al., "Effects of bedding plane on anthracite coal resistivity under different temperatures," *Chinese Journal of Engineering*, vol. 39, no. 7, pp. 988–995, 2017.

[15] J. Shen and N.–C. Guo, "Study on apparent resistivity and magnetic field response in anisotropic layered media," *Chinese Journal of Rock Mechanics and Engineering*, vol. 51, no. 5, pp. 1608–1619, 2008.

[16] B. Deng, X. Kang, X. Li et al., "Effect of different bedding directions on deformation and seepage characteristics of raw coal," *Journal of China Coal Society*, vol. 40, no. 4, pp. 888–894, 2015.

[17] Y. Tan, Z. Pan, J. Liu et al., "Experimental study of impact of anisotropy and heterogeneity on gas flow in coal. Part II: permeability," *Fuel*, vol. 230, pp. 397–409, 2018.

[18] K. Liu, Q. Liu, Y. Zhu et al., "Experimental study on Brazilian splitting and uniaxial compression of coal-rock considering the direction direction effect," *Chinese Journal of Rock Mechanics and Engineering*, vol. 32, no. 2, pp. 308–316, 2013.

[19] Z. Zhang, R. Zhang, G. Li, H. Li, and J. Liu, "The effect of bedding structure on mechanical property of coal," *Advances in Materials Science and Engineering*, vol. 2014, Article ID 952703, 7 pages, 2014.

[20] P. Chen, E. Wang, X. Chen, Z. Liu, Z. Li, and R. Shen, "Regularity and mechanism of coal resistivity response with different conductive characteristics in complete stress-strain process," *International Journal of Mining Science and Technology*, vol. 25, no. 5, pp. 779–786, 2015.

[21] L. Meng, M. Liu, and Y. Wang, "Experimental study on the change law of resistivity under uniaxial compression of structural coal," *Journal of China Coal Society*, vol. 35, no. 12, pp. 2028–2032, 2010.

[22] B. Nie, X. Liu, L. Yang, J. Meng, and X. Li, "Pore structure characterization of different rank coals using gas adsorption and scanning electron microscopy," *Fuel*, vol. 158, pp. 908–917, 2015.

[23] B. Fu, G. Liu, Y. Liu, S. Cheng, C. Qi, and R. Sun, "Coal quality characterization and its relationship with geological process of the early Permian Huainan coal deposits, southern North China," *Journal of Geochemical Exploration*, vol. 166, no. 7, pp. 33–44, 2016.

[24] Y. Cai, D. Liu, Z. Pan, Y. Yao, and C. Li, "Mineral occurrence and its impact on fracture generation in selected Qinshui Basin coals: an experimental perspective," *International Journal of Coal Geology*, vol. 150-151, pp. 35–50, 2015.

[25] P. Chen and X. Tang, "The research on the adsorption of nitrogen in low temperature and micro-pore properties in coal," *Journal of China Coal Society*, vol. 26, no. 5, pp. 552–556, 2001.

[26] S. J. Gregg, "Sixty years in the physical adsorption of gases," *Colloids and Surfaces*, vol. 21, pp. 109–124, 1986.

[27] F. Lu, J. Gao, J. Liu, X. Zhang, C. Wang, and Y. Liu, "Characterization of the coal pore system by resistivity and NMR methods," *Energy Sources, Part A: Recovery, Utilization, and Environmental Effects*, pp. 1–14, 2019.

[28] G. Zhang, X. Tan, X. Xie, and Y. Du, "Experimental study on the relationship between coal conductivity and coal macromolecular structure," *Coal Conversion*, vol. 17, no. 2, pp. 10–13, 1994.

[29] S. Liu, X. Li, D. Wang, M. Wu, G. Yin, and M. Li, "Mechanical and acoustic emission characteristics of coal at temperature impact," *Natural Resources Research*, vol. 28, no. 3, pp. 1755–1772, 2020.

[30] E.-Y. Wang, P. Chen, Z. Li, R.-X. Shen, J.-K. Xu, and Y.-F. Zhu, "Resistivity response in complete stress-strain process of loaded coal," *Journal of China Coal Society*, vol. 39, no. 11, pp. 2220–2225, 2014.

[31] J. Kang, "Study on the relationship between coal conductivity and crustal stress," *Journal of Henan Polytechnic University (Natural Science)*, vol. 24, no. 6, pp. 430–433, 2005.

[32] S. E. Laubach, R. A. Marrett, J. E. Olson, and A. R. Scott, "Characteristics and origins of coal cleat: a review," *International Journal of Coal Geology*, vol. 35, no. 1–4, pp. 175–207, 1998.

[33] F. Lu, Y. Zhang, and L. Jiang, "Anisotropic characteristics of nuclear magnetic resonance of pores and fractures in coal under uniaxial loading," *Coal Geology & Exploration*, vol. 46, no. 1, pp. 66–72, 2018.

[34] Y. Chen, X. Su, J. Wang et al., *Petroleum Geology and Recovery Efficiency*, vol. 26, no. 5, pp. 66–72, 2019.

[35] Y. Wan, Z. Pan, S. Tang, L. D. Connell, D. D. Down, and M. Camilleri, "An experimental investigation of diffusivity and porosity anisotropy of a Chinese gas shale," *Journal of Natural Gas Science and Engineering*, vol. 23, pp. 70–79, 2015.

[36] S. Peng, "Study on the mechanism of failure and instability of gas bearing coal and its application," Chongqing University, Chongqing, China, Ph.D. dissertation, 2011.
[37] L. Zhong, "The cause of internal cracks in coal," *Coal Geology of China*, vol. 16, no. 3, pp. 6–9, 2004.
[38] Y. Du, Z. Ren, X. Xian et al., "Relationship between the anisotropy of coal and its macromolecular structure," *Coal Conversion*, vol. 18, no. 4, pp. 63–67, 1995.
[39] X. Fu, *Theory and Method for Predicting Permeability of Coalbed Methane Reservoirs in Multiphase Media*, China University of Mining and Technology, Xuzhou, China, 2003.
[40] Y. Liu, D. Tang, H. Xu et al., "Characteristics of the stress deformation of pore-fracture in coal based on nuclear magnetic resonance," *Journal of China Coal Society*, vol. 40, no. 6, pp. 1415–1421, 2015.
[41] H. Deng, W. Wang, J. Li et al., "Experimental study on anisotropic mechanical properties of layered sandstone," *Chinese Journal of Rock Mechanics and Engineering*, vol. 37, no. 1, pp. 112–120, 2018.
[42] W. Jin, *Dielectric Physics*, Science Press, Beijing, China, 2003.
[43] P. Chen, E.-Y. Wang, and Y.-F. Zhu, "Experimental study on resistivity variation regularities of loading coal," *Journal of China Coal Society*, vol. 38, no. 4, pp. 548–553, 2013.
[44] S. Bi, H. Zhang, Y. Zhang et al., "Experimental study on coal resistivity changing anisotropy during uniaxial compression," *Safety in Coal Mines*, vol. 47, no. 12, pp. 35–38, 2016.